



OPEN

Molecular characteristics and stable carbon isotope compositions of dicarboxylic acids and related compounds in wintertime aerosols of Northwest China

Weining Qi¹, Gehui Wang², Wenting Dai¹, Suixin Liu¹, Ting Zhang¹, Can Wu², Jin Li¹, Minxia Shen¹, Xiao Guo¹, Jingjing Meng³✉ & Jianjun Li^{1,4,5}✉

Dicarboxylic acids are one of the important water-soluble organic compounds in atmospheric aerosols, causing adverse effects to both climate and human health. More attention has therefore been paid to organic acids in aerosols. In this study, the molecular distribution and diurnal variations of wintertime dicarboxylic acids in a rural site of Guanzhong Plain, Northwest China, were explored. Oxalic acid (C₂, day: 438.9 ± 346.8 ng m⁻³, night: 398.8 ± 392.3 ng m⁻³) is the most abundant compound followed by methylglyoxal (mGly, day: 207.8 ± 281.1 ng m⁻³, night: 222.9 ± 231.0 ng m⁻³) and azelaic (C₉, day: 212.8 ± 269.1 ng m⁻³, night: 211.4 ± 136.7 ng m⁻³) acid. The ratios of C₉/C₆ and C₉/Ph indicating that atmospheric dicarboxylic acids in winter in the region mainly come from biomass burning. Furthermore, secondary inorganic ions (NO₃⁻, SO₄²⁻, and NH₄⁺), relative humidity, liquid water content, and *in-situ* pH of aerosols are highly linearly correlated with C₂, suggesting that liquid phase oxidation is an important pathway for the formation of dicarboxylic acids. The δ¹³C analysis of C₂ suggested that lighter carbon isotope compositions tend to be oxidized to form aqueous-phase secondary organic aerosols (aqSOA), leading to the decay of ¹³C in aqSOA products rather than aerosol aging. This study provides a theoretical basis for the mechanism of formation of dicarboxylic acid.

Secondary organic aerosols (SOAs), generated by physical and chemical transformation of volatile organic compounds (VOCs) as gaseous precursors in the atmosphere^{1,2}, are closely related to some natural phenomena such as solar radiation, particle growth, cloud condensation nuclei formation, and reduced visibility^{3,4}. Dicarboxylic acids, ketocarboxylic acids and α-dicarbonyls are important classes of SOAs, which mainly produced from photochemical oxidation with ozone or hydroxyl radicals (•OH)⁵ and aqueous processing⁶. Dicarboxylic acids and related polar organic compounds, water-soluble organic carbons (WSOC), can be always detected in urban⁷, mountain⁸, and remote region⁹. In addition, dicarboxylic acid is generally considered as an indicator of the degree of oxidation of WSOC in the atmosphere^{10–12}, so it is quite necessary to explore the composition, source and oxidation mechanism of dicarboxylic acid in the atmosphere.

Domestic and foreign studies on the composition and source of dicarboxylic acid are mainly based more on the seasonal variations and trends therein in urban atmospheric aerosol^{13,14} but the diurnal variation of dicarboxylic acid in the rural of Northwest China is rarely studied. Guanzhong Plain, located in Northwest China, is one of the most heavily polluted regions in China with an annual average PM_{2.5} of more than 80 μg m⁻³¹⁵. It was reported that high levels of PM_{2.5} have a significant damaging effect on atmospheric visibility and human health¹⁶ in which water-soluble SOAs may play the vital roles since it not only scatters or absorbs visible light but amplifies the pollution solubility in the respiratory tract¹⁷. It is important to understand the source of water-soluble organic

¹State Key Laboratory of Loess and Quaternary Geology, Key Lab of Aerosol Chemistry and Physics, Institute of Earth Environment, Chinese Academy of Sciences, Xi'an 710061, China. ²Key Laboratory of Geographic Information Science of the Ministry of Education, School of Geographic Sciences, East China Normal University, Shanghai 200241, China. ³School of Geography and the Environment, Liaocheng University, Liaocheng 252000, China. ⁴CAS Center for Excellence in Quaternary Science and Global Change, Xi'an 710061, China. ⁵National Observation and Research Station of Regional Ecological Environment Change and Comprehensive Management in the Guanzhong Plain, Xi'an, Shaanxi, China. ✉email: lijing@ieecas.cn; mengjingjing@lcu.edu.cn

compounds. Stable carbon isotope analysis can provide available information about the sources and composition and formation mechanism of organic aerosols¹⁸. Therefore, isotope analysis, widely used, focuses on urban areas, such as Beijing^{18,19} and Xi'an to explore the source of atmospheric organic aerosols²⁰. However, isotope analysis is rarely used to analyze the source and distribution of dicarboxylic acids in rural areas.

In this study, we measured dicarboxylic acids, ketocarboxylic acids, and α -dicarbonyls which collected in the rural area of Guanzhong Plain to study their sources and mechanisms of formation. The objectives of the present study are: (1) identify the source and composition of dicarboxylic acid in PM_{2.5} of atmospheric organic aerosol in the rural area of Northwest China; (2) assess the diurnal variations of these dicarboxylic acids and (3) reveal the mechanism of formation of dicarboxylic acid and related SOAs.

Sampling and analysis

Sample collection. In Lincun (34° 44' N and 109° 32' E, 354 m a.s.l.), a small village, is distancing 40 km northeast of Xi'an, the capital of Shaanxi Province, China. We collected PM_{2.5} samples from 20 January to 1 February during the winter in 2017. The aerosol sampler was located in the rooftop of a three-storey building. PM_{2.5} samples were collected by a mid-volume air sampler (Laoshan Company, China) at an airflow rate of 100 L min⁻¹ on a pre-baked (450 °C for 12 h) quartz fiber filter (Φ 90 mm) on a day (08:00–19:00)/night (20:00–07:00) basis for 10 h each half-cycle. At the beginning and the end of the sampling, field blank samples were collected by mounting the blank filter onto the sampler for 10 min without sucking air. The total samples were sealed within an aluminum foil bag and stored at –18 °C before the laboratory analysis²¹.

Sample analysis. *Dicarboxylic acids and related organic compounds.* Dicarboxylic acids, ketocarboxylic acids, and α -dicarbonyls were analyzed and the methods can be found anywhere^{22,23}. In short, firstly, Milli-Q water extracted ultrasonically a quarter of the filtrate three times. Then, under vacuum condition, the sample was concentrated to dryness by rotary evaporation and reacted with 14% BF₃/butanol mixture at 100 °C for 1 h. Thereafter, the sample was derivatized and added to n-hexane, extracted by pure water three times. Finally, the hexane layer was concentrated to 100 μ L by nitrogen blowing and quantified by gas chromatography (GC) (Agilent, GC7890A) coupled with an FID detector (DB-5MS, 30 m \times 1.25 mm \times 0.25 m).

The temperatures of GC oven was programmed to ascend from 50 to 120 °C at a gradient of 30 °C min⁻¹, and then at a rate of 6 °C min⁻¹ to 300 °C and hold at 300 °C for 10 min. The target compounds recoveries of oxalic acid could reach to 80–85% and 92–115% for others. In the field blanks, target compounds were less than 5% of those in actual specimens. Data reported here were corrected by use of field blank specimens but not by the recoveries.

Stable carbon isotope composition of dicarboxylic acids and related SOAs. The shorter chain dicarboxylic acids and related SOAs could be measured by the stable carbon isotopic compositions ($\delta^{13}\text{C}$), described by Aggarwal and Kawamura²². Briefly, the samples $\delta^{13}\text{C}$ values were detected by gas chromatography–isotope ratio mass spectrometry (GC-IR-MS; Thermo Fisher, Delta V Advantage). Then, based on the measured $\delta^{13}\text{C}$ values of derivatives and the derivatizing agent (BF₃ = n-butanol) we used isotopic mass balance equation to calculate the $\delta^{13}\text{C}$ values of free organic acids²⁴. We measured three times for every sample to ensure the analytical error of the $\delta^{13}\text{C}$ values less than 0.2‰. The $\delta^{13}\text{C}$ data reported here are averaged values of the triplicate measurements.

Carbonaceous fractions and water-soluble inorganic ions. Elemental carbon (EC) and organic carbon (OC) were applied by a DRI Model 2001 Carbon Analyzer following the Interagency Monitoring of Protected Visual Environments (IMPROVE) Thermal/Optical Reflectance (TOR) protocol performed by Yang²⁵. Inorganic ions and water-soluble organic carbons was extracted by the conventional method as detailed elsewhere²⁶. Besides, the liquid water content (LWC) and *in-situ* (pH_{is}) of particles were calculated by ISORROPIA-II²⁷.

Results and discussion

Overview of meteorological conditions and chemical components. Diurnal variations of meteorological parameters and the determined dicarboxylic acids (α -dicarbonyls, keto-carboxylic acids and dicarboxylic acids) are illustrated in Fig. 1. During the sampling periods, relative humidity (RH), PM_{2.5} concentrations and LWC reach their peak (Fig. 1A,C,D) while wind speeds (WSs) (Fig. 1B) are lowest. As shown in Table 1, the mass concentration of PM_{2.5} ranged from 54.0 to 430.6 $\mu\text{g m}^{-3}$, with mean values of 189.8 \pm 91.7 and 181.1 \pm 107.6 $\mu\text{g m}^{-3}$ in day-time and night-time, respectively. It was much higher than the national air quality standard of 75 $\mu\text{g m}^{-3}$, indicating serious air pollution in the rural region of Northwest China. OC and EC were 44.0 \pm 17.9 and 13.6 \pm 6.8 $\mu\text{g m}^{-3}$ by day and 47.9 \pm 28.4 and 14.1 \pm 5.3 $\mu\text{g m}^{-3}$ by night, respectively. Our results were lower than those measured in Xi'an (OC: 59 \pm 28, EC: 19 \pm 8.2)²⁸. The OC/EC was 3.1 \pm 0.3 $\mu\text{g m}^{-3}$ by day and 3.4 \pm 0.4 $\mu\text{g m}^{-3}$ by night, indicating almost no difference between day and night. The LWC values were 21.2 \pm 20.83 (day) and 33.86 \pm 46.74 $\mu\text{g m}^{-3}$ (night), which were significantly lower than those of LWC (94 \pm 100 $\mu\text{g m}^{-3}$ by day and 75 \pm 69 $\mu\text{g m}^{-3}$ by night) at top Mount Tai, which was possibly due to the high RH at its summit. pH_{is} values were 3.43 \pm 3.36 and 3.65 \pm 1.89 $\mu\text{g m}^{-3}$ by day and night, respectively.

Concentrations of total dicarboxylic acids (940.3 \pm 967.8 ng m⁻³), keto-carboxylic acids (128.8 \pm 73.7 ng m⁻³), and α -dicarbonyls (229.5 \pm 294.1 ng m⁻³) by day were higher than those (903.8 \pm 727.1, 111.6 \pm 72.6, and 223.7 \pm 243.5 ng m⁻³) by night. The concentrations of total dicarboxylic acids and related SOAs fluctuated significantly, with a maximum (2161 ng m⁻³) on 24 and 25 Jan, 2017 and minimum (37.6 ng m⁻³) on 31 Jan. (Fig. 2B). Dicarboxylic acid increased with the increase of LWC, suggesting enhanced formation of dicarboxylic acid through liquid oxidation in (Fig. 1D), while high pH is not conducive to the formation of dicarboxylic acid. This result was consistent with previous research results^{29,30}. α -dicarbonyls and keto-carboxylic also exhibited the

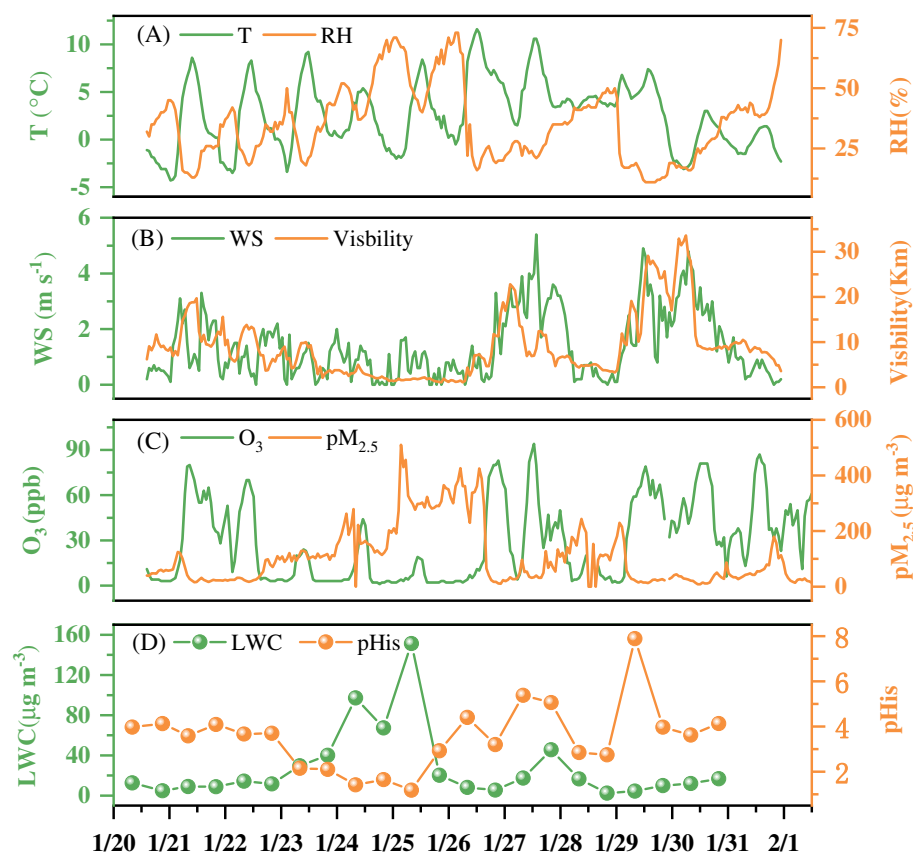


Figure 1. Diurnal variations of temperature (T), relative humidity (RH), wind speed (WS), visibility concentrations of O_3 , $PM_{2.5}$, liquid water content (LWC) and pHHis.

same fluctuating trend as dicarboxylic acid in Fig. 2A and C. We found that high RH and low WS are beneficial to the transformation and generation of Dicarboxylic acid. The minimum WS is not conducive to the migration and diffusion of dicarboxylic acids, leading to the accumulation of SOAs³¹. The results indicated that atmospheric meteorological parameters are closely related to the change of dicarboxylic acids in the environment, and our experimental results verify the previous research conclusions³².

On 28 Jan. (the traditional Chinese Spring Festival), the concentration of dicarboxylic acid was significantly reduced. Meanwhile, the concentrations of K^+ , Ca^{2+} , and Mg^{2+} were 22.53 , 2.81 , and $0.74 \mu g m^{-3}$, respectively in Table 2, reaching their maxima³¹. Metal ions such as K^+ , Ca^{2+} , and Mg^{2+} were common in fireworks³³. During the festival, local residents set off fireworks containing metal ions, which could be released into the atmosphere and react with the dicarboxylic acids to form a stable complex (such as calcium oxalate). Therefore, the content of dicarboxylic acid decreased significantly during Spring Festival. Our results are similar to those reported in previous studies³⁴.

The molecular composition of dicarboxylic acids and its related compounds. The molecular composition of dicarboxylic acids and related compounds is demonstrated in Fig. 3. C_2 , (day: $438.9 \pm 346.8 ng m^{-3}$, night $398.8 \pm 392.3 ng m^{-3}$) is the most abundant dicarboxylic acid, followed by methylglyoxal (mGly), azelaic acid, and phthalic acid (Ph, day: $68.2 \pm 28.8 ng m^{-3}$, night: $63.6 \pm 33.1 ng m^{-3}$) in dicarboxylic acids. The concentrations of C_9 are $212.8 \pm 269.1 ng m^{-3}$ and $211.4 \pm 136.7 ng m^{-3}$ by day and by night. In addition, mGly contents by day ($207.8 \pm 281.1 ng m^{-3}$) are equal to those at night ($222.9 \pm 231.0 ng m^{-3}$), accounting for more than 90% of the total α -dicarbonyls. Gly concentrations at $21.7 \pm 15.3 ng m^{-3}$ by day and $19.4 \pm 15 ng m^{-3}$ by night are significantly lower than those of mGly. The reason for this may be that, compared with Gly, mGly has stronger biogenic sources and the lower oxidation rate of with OH radicals in the aerosol phase^{35,36}. These α -dicarbonyls may serve as precursors to SOAs through heterogeneous reactions³⁷. Ketoacids (day: $60.3 \pm 35.1 ng m^{-3}$, night: $52.0 \pm 34.5 ng m^{-3}$) are dominant in the keto-carboxylic acids. Ranked second is glyoxylic acid (ωC_2) at $44.9 \pm 31.2 ng m^{-3}$ by day and $37.1 \pm 30.6 ng m^{-3}$, by night, respectively. It was reported that ωC_2 is originally formed from glyoxal photochemically oxidized with OH radicals and other oxidants in the aqueous phase, followed by further oxidation to oxalic acid^{21,38}.

Possible sources and mechanism of formations of dicarboxylic acids and related compounds. The characteristic ratios can be used to investigate the sources and formation process of dicarboxylic acids and related compounds³⁹. Ratios of, C_2/C_4 , C_3/C_4 , C_9/C_6 , C_9/Ph , C_2/TD , Gly/mGly, and OC/EC

	Day (n = 12)	Night (n = 12)
<i>I. Dicarboxylic acids, ng m⁻³</i>		
Oxalic, C ₂	438.9 ± 346.8	398.8 ± 392.3
Malonic, C ₃	39.5 ± 36.6	35.8 ± 35.3
Succinic, C ₄	57.9 ± 33.4	59.6 ± 47.1
Glutaric, C ₅	15.8 ± 10.4	16.6 ± 13.6
Adipic, C ₆	10.0 ± 4.1	9.7 ± 5.8
Pimelic, C ₇	10.9 ± 5.6	10.2 ± 7.7
Suberic, C ₈	7.2 ± 4.3	7.5 ± 5.9
Azelaic, C ₉	212.8 ± 269.1	211.4 ± 136.7
Undecanedioic, C ₁₀	38.2 ± 43.2	30.4 ± 26.8
Undecanedioic, C ₁₁	6.7 ± 3.8	6.6 ± 5.3
Methylsuccinic, iC ₅	9.5 ± 6.0	9.1 ± 7.4
Methylglutaric, iC ₆	7.9 ± 10.3	8.0 ± 10.6
Maleic, M	6.7 ± 11.0	9.3 ± 16.1
Fumaric, F	8.9 ± 7.3	8.5 ± 7.2
Phthalic, Ph	68.2 ± 28.8	63.6 ± 33.1
Isophthalic, iPh	5.8 ± 3.9	6.4 ± 6.3
Terephthalic, tPh	3.2 ± 2.4	4.6 ± 3.7
Subtotal	940.3 ± 967.8	903.8 ± 727.1
<i>II. Keto-carboxylic acids, ng m⁻³</i>		
Pyruvic, Pyr	15.4 ± 6.6	14.9 ± 4.9
Glyoxylic, ωC ₂	44.9 ± 31.2	37.1 ± 30.6
7-Oxoheptanoic, ωC ₇	8.3 ± 4.6	7.5 ± 4.5
Ketoacids	60.3 ± 35.1	52.0 ± 34.5
Subtotal	128.8 ± 73.7	111.6 ± 72.6
<i>III. α-Dicarbonyls, ng m⁻³</i>		
Glyoxal, Gly	21.7 ± 15.3	19.4 ± 15.1
Methylglyoxal, mGly	207.8 ± 281.1	222.9 ± 231.0
Subtotal	229.5 ± 294.1	223.7 ± 243.5
<i>IV. Others, μg m⁻³</i>		
OC	44.0 ± 17.9	47.9 ± 28.4
EC	13.6 ± 6.8	14.1 ± 5.3
PM _{2.5}	189.8 ± 91.7	181.1 ± 107.6
LWC	21.2 ± 20.83	33.86 ± 46.74
pHis	3.43 ± 3.36	3.65 ± 1.89
<i>V. Carbon isotope</i>		
δ ¹³ C	-20.50 ± 3.30	-19.94 ± 3.61

Table 1. Concentrations of dicarboxylic acids, keto-carboxylic acids, α-dicarbonyls, OC, and EC in PM_{2.5} of Weinan, China by day and night.

are displayed in Fig. 4. C₂ is formed by photochemical oxidation of various precursors with hydroxyl radicals ($\cdot\text{OH}$)⁴⁰. C₄ is hydroxylated to form hydroxy succinic acid (*hC*₄), which can further form C₂ and C₃¹⁴. The ratio of C₃/C₄ is useful for evaluation of photochemical oxidation degree since C₃ is produced from C₄ by photochemical oxidation. Thus, the ratios of C₂/C₄ and C₃/C₄ are used to characterize the photochemical oxidation of organic aerosols⁴¹. The ratio of C₂/C₄ is 7.8 ± 1.70 by day and 6.4 ± 0.35 by night, respectively, similar to those in a mountainous atmosphere (8.0 ± 2.7)⁴², lower than those in the North and South Pacific (8.7)⁴³, and higher than that from vehicle exhausts (4.1)²¹. The C₃/C₄ ratio does not differ much between day (0.62 ± 0.22) and night (0.53 ± 0.27), but was significantly lower than on the Tibetan Plateau (2.2 ± 1.3) in summer³⁵. A strong correlation between C₃/C₄ and ambient temperature has been reported, proving that high temperatures contribute to the photochemistry of organic aerosols⁴⁴. However, such correlation is not found in this study. C₂/TD was similar by day (0.47 ± 0.05) and night (0.4 ± 0.16). These results suggest that photochemical aging is insignificant.

Previous study found that C₆ and Ph are mainly produced by the oxidation of anthropogenic cyclohexene and aromatic hydrocarbons^{45,46}. On the contrary, C₉ is mainly produced by the oxidation of biogenic unsaturated oleic acid, which contains a double bond at the C-9 position⁴⁷. Thus, both ratios of C₉/C₆ and C₉/Ph are indicative of the source strengths of biogenic *versus* anthropogenic emissions. The ratio of C₉/C₆ is higher by night (21.75 ± 5.61) than by day (19.37 ± 20.25), which is related to the higher emissions from biomass burning sources in rural areas by night. The ratios of C₉/Ph are 2.75 ± 2.36 (day), and 3.23 ± 1.32 (night), respectively. Our results

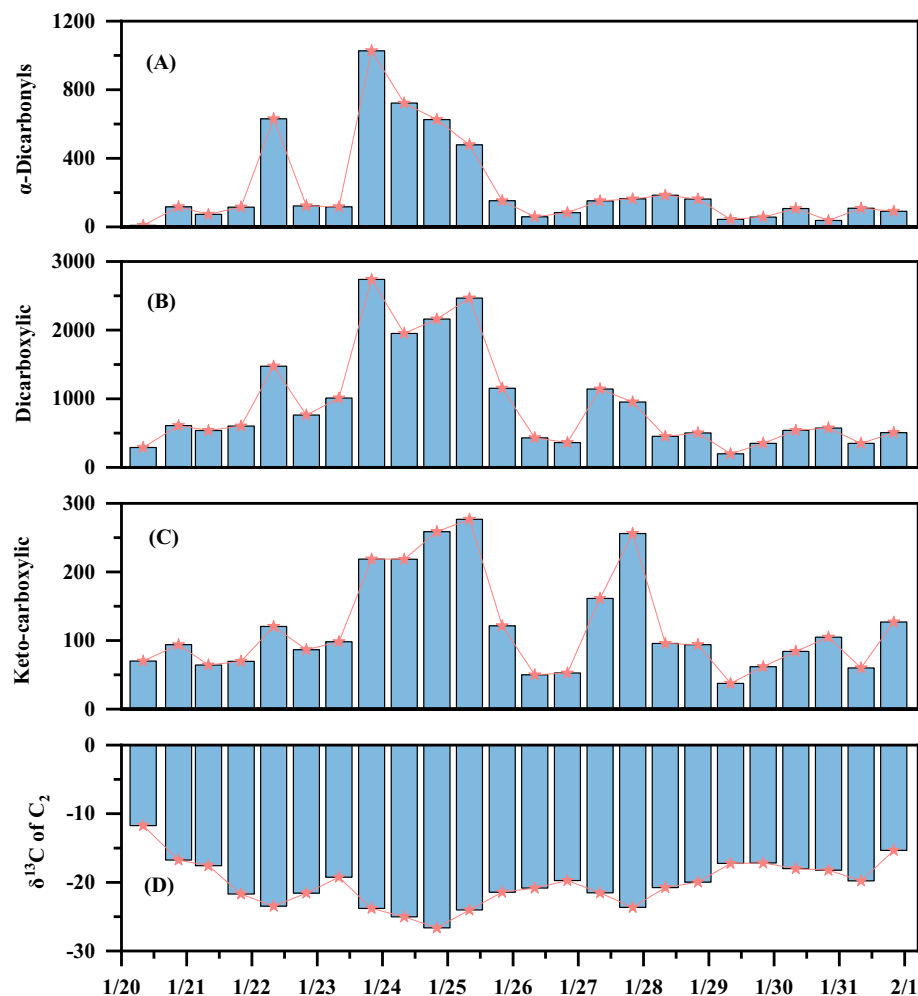


Figure 2. Diurnal variations of α -dicarbonyls, keto-carboxylic acids, and dicarboxylic acids.

Ions	K ⁺	Ca ²⁺	Mg ²⁺
Concentration ($\mu\text{g m}^{-3}$)	22.53	2.81	0.74

Table 2. Concentrations of K⁺, Ca²⁺, and Mg²⁺.

are lower than those measured at top Mount Tai (7.2 ± 2.2) in summer²¹. It is more likely that the photochemical reaction of unsaturated fatty acids emitted by biological sources on Mount Tai in summer is more intense than that in the rural regions investigated during this study in winter.

The ratios of Gly/mGly produced by anthropogenic and biological sources are 1:1 and 1:5, respectively⁴⁸. Since the absorption coefficients of Gly and mGly are similar, when the biological source is a single emission source, the ratio of Gly/mGly should theoretically be 1:5. In contrast, when the anthropogenic source is a single emission source, Gly/mGly should be 1:1. In this study, the Gly/mGly ratio is 0.18 ± 0.15 by day and 0.12 ± 0.05 by night, which was close to 1:5. However, as discussed above, as well as previous studies conducted in Guanzhong Plain, anthropogenic emission from biomass and/or fossil fuel combustion was considered as the predominant source of atmospheric aerosols in winter in the region. These results may suggest that mGly have another source or formation processes other than biological emission, and the exact explanation needs further research.

The linear relationships between C₂ and inorganic ions (NO₃⁻, SO₄²⁻, and NH₄⁺), meteorological parameters (LWC, RH, O₃, and pH_{is}) and ωC_2 , are shown in Fig. 5. NO₃⁻, SO₄²⁻, and NH₄⁺ play a critical role in the formation of dicarboxylic acid⁴⁹. The linear correlation coefficient between NO₃⁻ and C₂ is 0.90, indicating a positive correlation between them (Fig. 5A). Our results are in accord with those of a previous study⁵⁰. In Fig. 5B, SO₄²⁻ also shows a similar effect, and the correlation coefficient between SO₄²⁻ and C₂ is 0.81. The sulphates (SO₄²⁻) in the atmosphere mainly come from the liquid-phase oxidation of SO₂ emitted from coal burning on the surface of fine particles⁵¹, as favored by high-temperature, humid conditions⁵². The results confirm that C₂ is mainly formed by liquid oxidation. In addition, NH₄⁺ also has a high linear correlation in Fig. 5C, with r^2 reaching 0.88. This

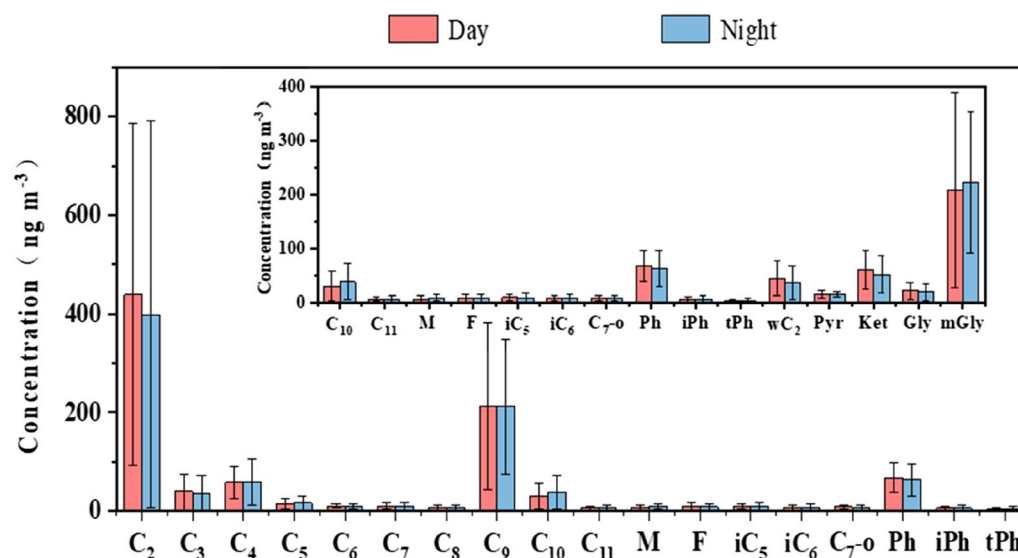


Figure 3. Molecular compositions of dicarboxylic acids and related compounds in $PM_{2.5}$ over Weinan.

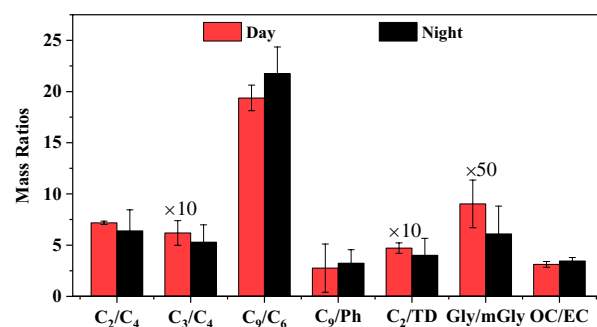


Figure 4. Diurnal variations of mass ratios of C_2/C_4 , C_3/C_4 , C_9/C_6 , C_9/Ph , C_2/TD , $Gly/mGly$, and OC/EC (TD: total dicarboxylic acids; the mass ratios of C_2/TD , C_3/C_4 , and $Gly/mGly$ expanding 10 and 50 times, respectively).

indicates that alkaline conditions are more conducive to the formation of C_2 . Consistent with the reaction results, alkalinity gradually increased with the decrease of acidity of atmospheric particles, contributing to the transformation of dicarboxylic acid precursor to C_2 ⁵³. NO_x will form NO_3^- in the liquid film through heterogeneous reaction, and then absorb NH_4^+ in the air. Nitrate on the surface of particulate matter will further enhance the water absorption of atmospheric particles, expand the liquid phase on the surface, and provide a possibility for the dissolution and reaction of SOAs⁵⁴. Therefore, our earlier studies proved that dicarboxylic acids are mainly derived through SOA formation via reactions in aqueous phase^{55,56}.

In Fig. 5D, the r^2 value of LWC is 0.81, indicating that C_2 is mainly produced by the distribution of precursor from gas to liquid phase and the subsequent liquid phase process. The increase in LWC contributes to the generation of SOAs⁵⁷. In addition, the LWC of atmospheric aerosol is mainly affected by RH and inorganic salt ions⁵⁸. C_2 is positively correlated with RH, and its linear correlation coefficient is 0.75 (Fig. 5E). Previous studies show that RH and LWC have a linear relationship with the formation of C_2 , indicating that a wet environment is conducive to the formation of a C_2 aqueous phase^{30,59}. Our experimental results confirm the previous research again that the binary carboxylic acids in the atmosphere mainly come from liquid phase oxidation⁶. Glyoxylic acid (ωC_2) is an intermediate product of the liquid phase reaction of dicarboxylic acid. C_2 and ωC_2 have a good linear correlation, as illustrated in Fig. 5F, with a linear correlation coefficient of 0.87. The concentration of C_2 increases with the increase of the concentration of ωC_2 , again proving that oxalic acid is formed by liquid-phase oxidation.

There is a significant negative correlation between C_2 and O_3 and pH_{is} , and the linear correlation coefficients are only 0.29 and 0.37 in Fig. 5G and H, respectively. This reveals that the roles of O_3 and pH_{is} are not obvious in this research, however, as reported, O_3 is an oxidizing substance in the atmosphere, and increasing O_3 concentration is conducive to the transformation of primary pollutants into secondary pollutants⁶⁰. It may be that dicarboxylic acids and their compounds are transformed through liquid-phase oxidation, which may be related to other oxidants, such as H_2O_2 , HO radical and NO_3 radical. The acidity of organic aerosols was found to be related to the formation of biological SOAs⁶¹. C_2 is negatively correlated with pH_{is} , which is possibly because strongly

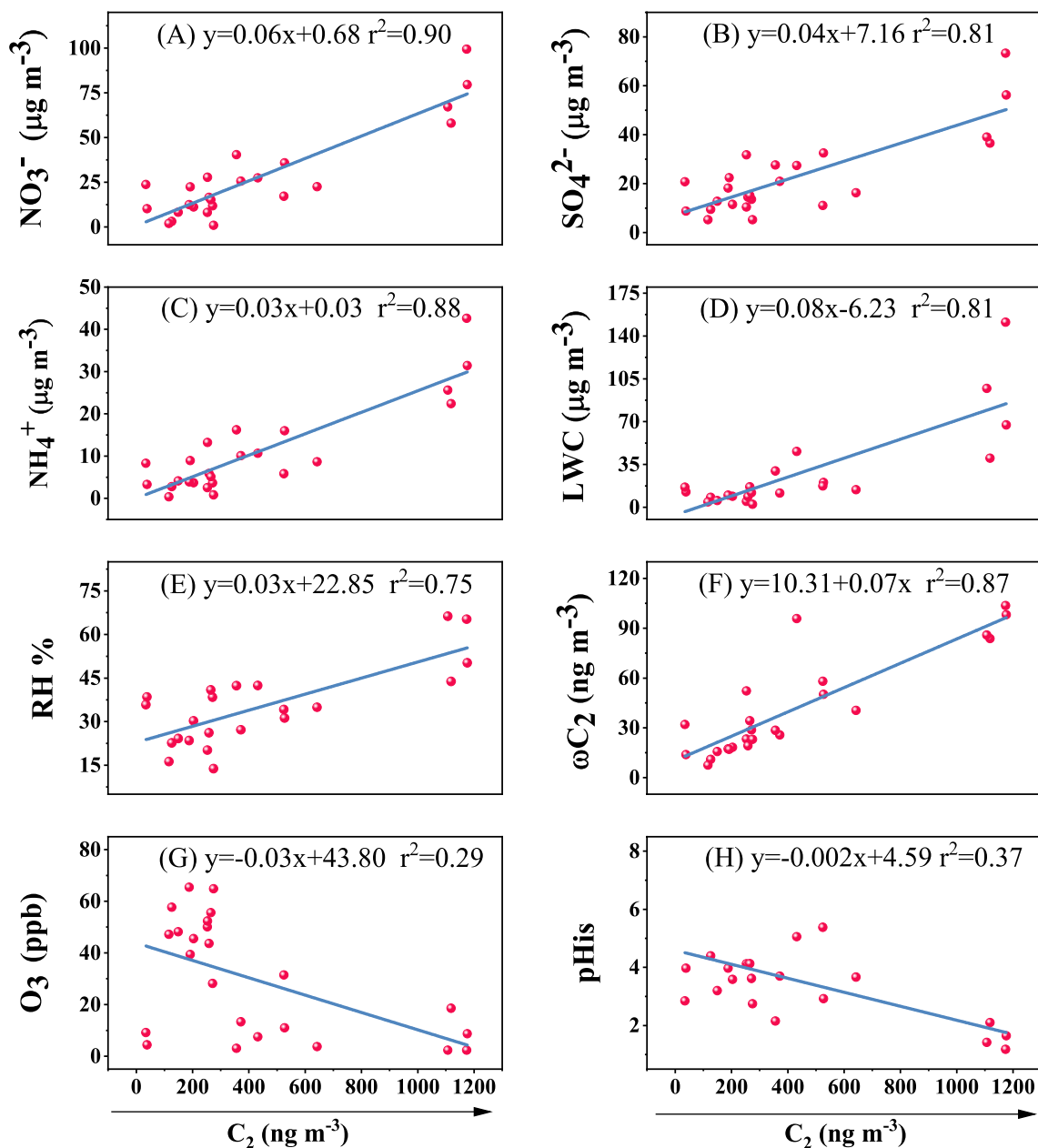


Figure 5. Linear regressions of oxalic acid (C_2) with NO_3^- , SO_4^{2-} , NH_4^+ , liquid water content (LWC), relative humidity (RH), O_3 , pH_{His}, and ωC_2 .

acidic conditions can inhibit the generation of dicarboxylic acid and its precursors. Furthermore, increasing RH can reduce the relative acidity, which is not conducive to the formation of dicarboxylic acid in acid catalytic reactions⁶².

Diurnal variations in stable carbon isotopes of major dicarboxylic acids and related compounds.

The further to understand the mechanism of formation of C_2 , the $\delta^{13}\text{C}$ value of organic dicarboxylic acid by using the isotope mass balance equation for analyzing the degree of aging of aerosols. The diurnal variations of stable carbon isotopes of C_2 are illustrated in Fig. 2D, with the day and night-time ranges of -20.50 ± 3.30 (-15.33 to -26.64‰) and -19.94 ± 3.61 (-11.73 to -25.03‰), respectively. The $\delta^{13}\text{C}$ of C_2 values of oxalic acid in Sapporo aerosol is the highest (-14.0 to -22.4‰ , mean: -18.8‰)²² and ranges from -20.5 to -10.1 at the Korea Climate Observatory at Gosan in winter⁵⁰. Our results match those arising from previous studies. The trend in the variations of C_2 isotope content is more negative in the first five days. The reason for this phenomenon is that in the process of SOAs generated by the oxidation of precursor VOC, carbon atoms with lighter isotopes in the gas phase tend to be oxidized and enter the aerosol phase in the form of reaction products, forming SOAs⁶³. Therefore, SOA formation causes the attenuation of ^{13}C in aerosols ($\delta^{13}\text{C}$ reduction). At the same time, as shown in Fig. 1D, LWC also reached its maximum value. Due to the dynamic isotope frac-

tionation effect, VOC and SVOC precursors with lighter carbon isotope compositions tended to be oxidized to form aqSOA, resulting in the decline of ^{13}C in aqSOA products⁶⁴. Thus, the liquid phase generation pathway of dicarboxylic acid in this study is $\text{VOC} \rightarrow \text{SVOCs} \rightarrow \text{Pyr} \rightarrow \omega\text{C}_2 \rightarrow \text{C}_2$. Subsequently, $\delta^{13}\text{C}$ gradually shows an upward trend on 28 Jan. This is probably because Chinese traditional festivals focus on setting off fireworks and firecrackers, releasing many pollutants including some reactive metals such as Ca and K. The emitted metals could react with dicarboxylic acid to form water-insoluble oxalates, which cannot be measured by the analyzing method in this study. This meant that the formation of secondary oxalic acid was relatively weaker, resulting its carbon isotopes rise slightly.

Conclusion

In this study, total dicarboxylic acids, keto-carboxylic acids, α -dicarbonyls, EC, OC, $\text{PM}_{2.5}$, LWC, and pH_{is} from 20 January to 1 February 2017 in a rural site on Guanzhong Plain, Northwest China were analyzed. The mass concentration of $\text{PM}_{2.5}$ in the atmospheric aerosol ranged from 54.0 to 430.6 $\mu\text{g m}^{-3}$, significantly exceeding the national standard. Total dicarboxylic acids and ketocarboxylic acids and α -dicarbonyls fluctuated regularly with LWC and RH. Molecular composition of dicarboxylic acids in the aerosol samples was characterized by the predominance of oxalic (C_2) acid, methylglyoxal (mGly), and azelaic (C_9) acid. The source of pollution from dicarboxylic acid was mainly biological as evinced by C_6/C_6 , C_9/Ph , and Gly/mGly. There was a significant correlation between C_2 and LWC, which proved that C_2 was mainly produced by the distribution of precursor from gas to liquid phase and the subsequent liquid-phase process. In addition, C_2 concentration increased with the increase in the concentration of ωC_2 , the intermediate product of the liquid-phase reaction, which also confirmed the importance of the liquid-phase formation of oxalic acid. NO_3^- , SO_4^{2-} , and NH_4^+ played an important role in the formation of C_2 and its related compounds. The C_2 isotope data implied that SOAs were caused by precursor VOC oxidation rather than photochemical cracking of long-chain diacids.

Data availability

The datasets used and/or analysed during the current study available from the corresponding author on reasonable request.

Received: 21 March 2022; Accepted: 21 June 2022

Published online: 04 July 2022

References

- Porter, W. C., Jimenez, J. L. & Barsanti, K. C. Quantifying atmospheric parameter ranges for ambient secondary organic aerosol formation. *ACS Earth Space Chem.* **5**, 2380–2397 (2021).
- Qin, Y. *et al.* Humidity dependence of the condensational growth of α -pinene secondary organic aerosol particles. *Environ. Sci. Technol.* **55**, 14360–14369 (2021).
- Cheng, C. *et al.* Size-resolved airborne particulate oxalic and related secondary organic aerosol species in the urban atmosphere of Chengdu, China. *Atmos. Res.* **161–162**, 134–142 (2015).
- Lim, H. J. & Turpin, B. J. Origins of primary and secondary organic aerosol in Atlanta? Results of time-resolved measurements during the Atlanta supersite experiment. *Environ. Sci. Technol.* **36**, 4489–4496 (2002).
- Leresche, F. *et al.* Photochemical aging of atmospheric particulate matter in the aqueous phase. *Environ. Sci. Technol.* <https://doi.org/10.1021/acs.est.1c00978> (2021).
- Chen, Y. *et al.* Low-molecular-weight carboxylic acids in the Southeastern U.S.: Formation, partitioning, and implications for organic aerosol aging. *Environ. Sci. Technol.* **55**, 6688–6699 (2021).
- van Pinxteren, C. N. D. & Herrmann, H. On the abundance and source contributions of dicarboxylic acids in size-resolved aerosol particles at continental sites in central Europe. *Atmos. Chem. Phys.* **13**, 32093–32131 (2014).
- Kawamura, K. *et al.* High abundances of water-soluble dicarboxylic acids, ketocarboxylic acids and α -dicarbonyls in the mountaintop aerosols over the North China Plain during wheat burning season. *Atmos. Chem. Phys.* **13**, 8285–8302 (2013).
- Wang, H. & Kawamura, K. Stable carbon isotopic composition of low-molecular-weight dicarboxylic acids and ketoacids in remote marine aerosols. *J. Geophys. Res. Atmos.* <https://doi.org/10.1029/2005JD006466> (2006).
- Ervens, B., Turpin, B. J. & Weber, R. J. Secondary organic aerosol formation in cloud droplets and aqueous particles (aqSOA): A review of laboratory, field and model studies. *Atmos. Chem. Phys. Discuss.* **11**, 22301–22383 (2011).
- Kimitaka Kawamura, S. B. A review of dicarboxylic acids and related compounds in atmospheric aerosols_molecular distributions, sources and transformation. *Atmos. Res.* **170**, 140–160 (2016).
- Armin, S. *et al.* Constraining the contribution of organic acids and AMSm/z44 to the organic aerosol budget: On the importance of meteorology, aerosol hygroscopicity, and region. *Geophys. Res. Lett.* **37**, 21807 (2010).
- Čapka, L., Mikuška, P. & Krůmal, K. Determination of dicarboxylic acids in atmospheric aerosols using continuous aerosol sampler with on-line connected ion chromatography system. *Atmos. Environ.* <https://doi.org/10.1016/j.atmosenv.2019.117178> (2020).
- Chandra, P. *et al.* Water-soluble organic carbon, dicarboxylic acids, ketoacids, and α -dicarbonyls in the tropical Indian aerosols. *J. Geophys. Res. Atmos.* <https://doi.org/10.1029/2009JD012661> (2010).
- Donkelaar, A. V. *et al.* Global estimates of ambient fine particulate matter concentrations from satellite-based aerosol optical depth: Development and application. *Environ. Health Perspect.* **118**, 847–855 (2010).
- Cao, J. *et al.* Fine particulate matter constituents and cardiopulmonary mortality in a heavily polluted Chinese city. *Environ. Health Perspect.* **120**, 373–378 (2012).
- Kroll, J. H. & Seinfeld, J. H. Chemistry of secondary organic aerosol: Formation and evolution of low-volatility organics in the atmosphere. *Atmos. Environ.* **42**, 3593–3624 (2008).
- Zhao, W. *et al.* Molecular distribution and compound-specific stable carbon isotopic composition of dicarboxylic acids, oxocarboxylic acids and α -dicarbonyls in $\text{PM}_{2.5}$ from Beijing, China. *Atmos. Chem. Phys.* **18**, 2749–2767 (2018).
- Wang, J. *et al.* Concentrations and stable carbon isotope compositions of oxalic acid and related SOA in Beijing before, during, and after the 2014 APEC. *Atmos. Chem. Phys.* **17**, 981–992 (2017).
- Wang, G. *et al.* Molecular distribution and stable carbon isotopic composition of dicarboxylic acids, ketocarboxylic acids, and α -dicarbonyls in size-resolved atmospheric particles from Xi'an City, China. *Environ. Sci. Technol.* **46**, 4783–4791 (2012).
- Meng, J. *et al.* Molecular distribution and stable carbon isotopic compositions of dicarboxylic acids and related SOA from biogenic sources in the summertime atmosphere of Mt. Tai in the North China Plain. *Atmos. Chem. Phys.* **18**, 15069–15086 (2018).

22. Aggarwal, S. G. & Kawamura, K. Molecular distributions and stable carbon isotopic compositions of dicarboxylic acids and related compounds in aerosols from Sapporo, Japan: Implications for photochemical aging during long-range atmospheric transport. *J. Geophys. Res.* <https://doi.org/10.1029/2007JD009365> (2008).
23. Wang, G. *et al.* Observation of atmospheric aerosols at Mt. Hua and Mt. Tai in central and east China during spring 2009—Part 2: Impact of dust storm on organic aerosol composition and size distribution. *Atmos. Chem. Phys.* **12**, 4065–4080 (2012).
24. Kawamura, K. & Watanabe, T. Determination of stable carbon isotopic compositions of low molecular weight dicarboxylic acids and ketocarboxylic acids in atmospheric aerosol and snow samples. *Anal. Chem.* **76**, 5762–5768 (2004).
25. Yang, L. *et al.* Collocated speciation of PM_{2.5} using tandem quartz filters in northern Nanjing, China: Sampling artifacts and measurement uncertainty. *Atmos. Environ.* **246**, 118066 (2021).
26. Huang, X. *et al.* Characterization of oxalic acid-containing particles in summer and winter seasons in Chengdu, China. *Atmos. Environ.* **198**, 133–141 (2019).
27. Li, J. *et al.* Molecular characteristics and diurnal variations of organic aerosols at a rural site in the North China Plain with implications for the influence of regional biomass burning. *Atmos. Chem. Phys.* **19**, 1–43 (2019).
28. Cheng, C. *et al.* Comparison of dicarboxylic acids and related compounds in aerosol samples collected in Xi'an, China during haze and clean periods. *Atmos. Environ.* **81**, 443–449 (2013).
29. Kunwar, B. *et al.* Dicarboxylic acids, oxocarboxylic acids and α -dicarbonyls in atmospheric aerosols from Mt. Fuji, Japan: Implications for primary emission versus secondary formation. *Atmos. Res.* **221**, 58–71 (2019).
30. Deshmukh, D. K. *et al.* Sources and formation processes of water-soluble dicarboxylic acids, ω -oxocarboxylic acids, α -dicarbonyls, and major ions in summer aerosols from eastern central India. *J. Geophys. Res. Atmos.* **122**, 3630–3652 (2017).
31. Li, J. *et al.* Optical properties and molecular compositions of water-soluble and water-insoluble brown carbon (BrC) aerosols in northwest China. *Atmos. Chem. Phys.* **20**, 4889–4904 (2020).
32. Mochizuki, T. *et al.* Distributions and sources of low-molecular-weight monocarboxylic acids in gas and particles from a deciduous broadleaf forest in northern Japan. *Atmos. Chem. Phys.* **19**, 2421–2432 (2019).
33. Liu, H. *et al.* Characteristics and source analysis of water-soluble inorganic ions in PM₁₀ in a typical mining city, Central China. *Atmosphere* **8**, 74 (2017).
34. Xing, L. *et al.* Seasonal and spatial variability of the OM/OC mass ratios and high regional correlation between oxalic acid and zinc in Chinese urban organic aerosols. *Atmos. Chem. Phys.* **13**, 4307–4318 (2013).
35. Meng, J. *et al.* Atmospheric oxalic acid and related secondary organic aerosols in Qinghai Lake, a continental background site in Tibet Plateau. *Atmos. Environ.* **79**, 582–589 (2013).
36. Fu, T. M. *et al.* Global budgets of atmospheric glyoxal and methylglyoxal, and implications for formation of secondary organic aerosols. *J. Geophys. Res. Atmos.* <https://doi.org/10.1029/2007JD009505> (2008).
37. He, N. *et al.* Diurnal and temporal variations of water-soluble dicarboxylic acids and related compounds in aerosols from the northern vicinity of Beijing: Implication for photochemical aging during atmospheric transport. *Sci. Total Environ.* **499**, 154–165 (2014).
38. Rapf, R. J. *et al.* pH dependence of the aqueous photochemistry of α -keto acids. *J. Phys. Chem. A* **121**, 8368–8379 (2017).
39. Kundu, S., Kawamura, K. & Lee, M. Seasonal variations of diacids, ketoacids, and α -dicarbonyls in aerosols at Gosan, Jeju Island, South Korea: Implications for sources, formation, and degradation during long-range transport. *J. Geophys. Res.* <https://doi.org/10.1029/2010jd013973> (2010).
40. Sorooshian, A. *et al.* On the source of organic acid aerosol layers above clouds. *Environ. Sci. Technol.* **41**, 4647–4654 (2007).
41. Yang, L., Ray, M. B. & Yu, L. E. Photooxidation of dicarboxylic acids—Part II: Kinetics, intermediates and field observations. *Atmos. Environ.* **42**, 868–880 (2008).
42. Kawamura, K. & Kaplan, I. R. Motor exhaust emissions as a primary source for dicarboxylic acids in Los Angeles ambient air. *Environ. Sci. Technol.* **21**, 105–110 (1987).
43. Hoque, M. M. M., Kawamura, K. & Uematsu, M. Spatio-temporal distributions of dicarboxylic acids, ω -oxocarboxylic acids, pyruvic acid, α -dicarbonyls and fatty acids in the marine aerosols from the North and South Pacific. *Atmos. Res.* **185**, 158–168 (2017).
44. Yu, X. Y., Cary, R. & Laulainen, N. Primary and secondary organic carbon downwind of Mexico City. *Atmos. Chem. Phys. Discuss.* **9**, 541–593 (2009).
45. Kalberer, M. *et al.* Aerosol formation in the cyclohexene-ozone system. *Environ. Sci. Technol.* **34**, 4894–4901 (2000).
46. Kawamura, K. & Yasui, O. Diurnal changes in the distribution of dicarboxylic acids, ketocarboxylic acids and dicarbonyls in the urban Tokyo atmosphere. *Atmos. Environ.* **39**, 1945–1960 (2005).
47. Wang, G. *et al.* Selected water-soluble organic compounds found in size-resolved aerosols collected from urban, mountain and marine atmospheres over East Asia. *Tellus B Chem. Phys. Meteorol.* **63**, 371–381 (2011).
48. Meng, J. *et al.* Seasonal characteristics of oxalic acid and related SOA in the free troposphere of Mt. Hua, central China: Implications for sources and formation mechanisms. *Sci. Total Environ.* **493**, 1088–1097 (2014).
49. Trebs, I. *et al.* The NH₄⁺–NO₃[–]–Cl[–]–SO₄^{2–}–H₂O aerosol system and its gas phase precursors at a pasture site in the Amazon Basin: How relevant are mineral cations and soluble organic acids? *J. Geophys. Res. Atmos.* <https://doi.org/10.1029/2004JD005478> (2005).
50. Zhang, Y. L. *et al.* Stable carbon isotopic compositions of low-molecular-weight dicarboxylic acids, oxocarboxylic acids, α -dicarbonyls, and fatty acids: Implications for atmospheric processing of organic aerosols. *J. Geophys. Res. Atmos.* **121**, 3707–3717 (2016).
51. Veli-Matti, K. *et al.* Interaction between SO₂ and submicron atmospheric particles. *Atmos. Res.* **54**, 41–57 (2000).
52. Wang, G. *et al.* Particle acidity and sulfate production during severe haze events in China cannot be reliably inferred by assuming a mixture of inorganic salts. *Atmos. Chem. Phys.* **18**, 1–23 (2018).
53. Sorooshian, A. *et al.* Particulate organic acids and overall water-soluble aerosol composition measurements from the 2006 Gulf of Mexico Atmospheric Composition and Climate Study (GoMACCS). *J. Geophys. Res. Atmos.* <https://doi.org/10.1029/2007JD008537> (2007).
54. Wang, G. H. *et al.* Evolution of aerosol chemistry in Xi'an, inland China, during the dust storm period of 2013—Part 1: Sources, chemical forms and formation mechanisms of nitrate and sulfate. *Atmos. Chem. Phys.* **14**, 17439–17478 (2014).
55. Bikkina, S. *et al.* High abundances of oxalic, azelaic, and glyoxylic acids and methylglyoxal in the open ocean with high biological activity: Implication for secondary OA formation from isoprene. *Geophys. Res. Lett.* **41**, 3649–3657 (2014).
56. Bikkina, S. *et al.* Seasonal and longitudinal distributions of atmospheric water-soluble dicarboxylic acids, oxocarboxylic acids, and α -dicarbonyls over the North Pacific. *J. Geophys. Res. Atmos.* **120**, 5191–5213 (2015).
57. Pun, B. & Seigneur, C. Investigative modeling of new pathways for secondary organic aerosol formation. *Atmos. Chem. Phys.* **7**, 2199–2216 (2007).
58. Liu, H. *et al.* Particles liquid water and acidity determine formation of secondary inorganic ions in Urumqi, NW China. *Atmos. Res.* <https://doi.org/10.1016/j.atmosres.2021.105622> (2021).
59. Bikkina, S., Kawamura, K. & Sarin, M. Secondary organic aerosol formation over coastal ocean: Inferences from atmospheric water-soluble low molecular weight organic compounds. *Environ. Sci. Technol.* **51**, 4347–4357 (2017).
60. Zhang, Z. *et al.* Evolution of surface O₃ and PM_{2.5} concentrations and their relationships with meteorological conditions over the last decade in Beijing. *Atmos. Environ.* **108**, 67–75 (2015).
61. Surratt, J. D. *et al.* Reactive intermediates revealed in secondary organic aerosol formation from isoprene. *Proc. Natl. Acad. Sci.* **107**, 6640–6645 (2010).

62. Du, C. Y. *et al.* Impact of ambient relative humidity and acidity on chemical composition evolution for malonic acid/calcium nitrate mixed particles. *Chemosphere* **276**, 130140 (2021).
63. Fisseha, R. *et al.* Stable carbon isotope composition of secondary organic aerosol from β -pinene oxidation. *J. Geophys. Res. Atmos.* <https://doi.org/10.1029/2008JD011326> (2009).
64. Pavuluri, C. M. & Kawamura, K. Evidence for ^{13}C -carbon enrichment in oxalic acid via iron catalyzed photolysis in aqueous phase. *Geophys. Res. Lett.* <https://doi.org/10.1029/2011GL050398> (2012).

Acknowledgements

This work was financially supported by the program from National Natural Science Foundation of China (No. 41977332), and the Strategic Priority Research Program of Chinese Academy of Sciences (No. XDB40000000). Jianjun Li also acknowledged the support of the Youth Innovation Promotion Association CAS (No. 2020407).

Author contributions

W.Q.: original draft, Visualization, Investigation and Data curation; G.W.: Writing—original draft; W.D.: Data curation; S.L.: Validation; T.Z.: Data curation; C.W.: Data curation; J.L.: Data curation; M.S.: Validation; X.G.: Data curation; J.M.: Supervision, Methodology; J.L.: Writing—original draft, Visualization, Investigation and Supervision.

Competing interests

The authors declare no competing interests.

Additional information

Correspondence and requests for materials should be addressed to J.M. or J.L.

Reprints and permissions information is available at www.nature.com/reprints.

Publisher's note Springer Nature remains neutral with regard to jurisdictional claims in published maps and institutional affiliations.



Open Access This article is licensed under a Creative Commons Attribution 4.0 International License, which permits use, sharing, adaptation, distribution and reproduction in any medium or format, as long as you give appropriate credit to the original author(s) and the source, provide a link to the Creative Commons licence, and indicate if changes were made. The images or other third party material in this article are included in the article's Creative Commons licence, unless indicated otherwise in a credit line to the material. If material is not included in the article's Creative Commons licence and your intended use is not permitted by statutory regulation or exceeds the permitted use, you will need to obtain permission directly from the copyright holder. To view a copy of this licence, visit <http://creativecommons.org/licenses/by/4.0/>.

© The Author(s) 2022